123
5-27-97 8S (1)

ANL-97/4

Ultrasonic Methods for Measuring Liquid Viscosity and Volume Percent of Solids

by S.-H. Sheen, H.-T. Chien, and A. C. Raptis

Argonne National Laboratory, Argonne, Illinois 60439
operated by The University of Chicago
for the United States Department of Energy under Contract W-31-109-Eng-38

Reproduced from the best available copy.

Available to DOE and DOE contractors from the
Office of Scientific and Technical Information
P.O. Box 62
Oak Ridge, TN 37831
Prices available from (423) 576-8401

Available to the public from the
National Technical Information Service
U.S. Department of Commerce
5285 Port Royal Road
Springfield, VA 22161

Distribution
Category:
Instrumentation
and Monitoring
Techniques
(UC-606)

ARGONNE NATIONAL LABORATORY
9700 South Cass Avenue
Argonne, Illinois 60439

ANL-97/4

ULTRASONIC METHODS FOR MEASURING LIQUID VISCOSITY AND VOLUME PERCENT OF SOLIDS

by

S.-H. Sheen, H.-T. Chien, and A. C. Raptis

Energy Technology Division

February 1997

Work sponsored by

U. S. DEPARTMENT OF ENERGY
Office of Environmental Management

Contents

Figures

Tables

Ultrasonic Methods for Measuring Liquid Viscosity and Volume Percent of Solids

S.-H. Sheen, H.-T. Chien and A. C. Raptis

ABSTRACT

This report describes two ultrasonic techniques under development at Argonne National Laboratory (ANL) in support of the tank-waste transport effort undertaken by the U.S. Department of Energy in treating low-level nuclear waste. The techniques are intended to provide continuous on-line measurements of waste viscosity and volume percent of solids in a waste transport line. The ultrasonic technique being developed for waste-viscosity measurement is based on the patented ANL viscometer. Focus of the viscometer development in this project is on improving measurement accuracy, stability, and range, particularly in the low-viscosity range (<30 cP). A prototype instrument has been designed and tested in the laboratory. Better than 1% accuracy in liquid density measurement can be obtained by using either a polyetherimide or polystyrene wedge. To measure low viscosities, a thin-wedge design has been developed and shows good sensitivity down to 5 cP. The technique for measuring volume percent of solids is based on ultrasonic wave scattering and phase velocity variation. This report covers a survey of multiple scattering theories and other phenomenological approaches. A theoretical model leading to development of an ultrasonic instrument for measuring volume percent of solids is proposed, and preliminary measurement data are presented.

1 INTRODUCTION

This report covers the first-year effort in developing ultrasonic sensors for in-situ monitoring of physical properties of radioactive tank waste. This project is supported by the U.S. Department of Energy (DOE) Office of Environmental Management (EM-50), under the focus area of characterization, monitoring, and sensor technology (CMST). An estimated 381,000 m^3/1.1 x 10^9 Ci of radioactive waste are stored in high-level waste tanks at the Hanford, Savannah River, Idaho National Engineering Laboratory, and West Valley facilities. These nuclear wastes have created one of the most complex waste management and cleanup problems facing the United States. Release of radioactive materials to the environment from underground waste tanks requires immediate cleanup and waste retrieval. Hydraulic mobilization with mixer pumps will be the

process used to retrieve waste slurries and salt cake from storage tanks. To ensure that transport lines in the hydraulic system will not plug, the physical properties of the slurries must be monitored. Characterization of a slurry flow requires reliable measurements of slurry density, mass flow, viscosity, and volume percent of solids. Such measurements are preferably made with on-line nonintrusive sensors that can provide continuous real-time monitoring. To date, available on-line instruments for solid/liquid mixed phase flows are limited, and the Coriolis-type mass-flow meter is probably the only sensor being used by the industry at present.

This program intends to develop on-line ultrasonic sensors for measuring viscosity and volume percent of solids. The proposed viscosity sensor is based on Argonne National Laboratory's (ANL's) patented viscometer [1] that measures both density and viscosity. But while the ANL viscometer has been demonstrated in the high-viscosity range (>100 cP), it lacks sensitivity in low-viscosity measurement. Because the typical viscosity of the tank waste is <30 cP, the focus of this developmental effort is on improving the ANL viscometer for low-viscosity measurement. Sensitivity of the ANL viscometer depends on the shear impedance of the transducer wedge; thus, the primary task is to evaluate different wedge materials. In this report, we summarize this evaluation and propose an optimal wedge design. The baseline technology of the viscometer and its limitations are also described.

To date, ultrasonic methods for measuring volume percent of solids in solid suspensions are based on measurements of either sound velocity [2] or attenuation [3]. Both approaches show some correlation with solid concentration but are limited to low concentrations (<15 vol.%). The solids concentration range of the tank waste is about ≈30 vol.%. Thus, current ultrasonic methods must be modified to cover the range. Although many theoretical models that deal with multiple scattering in dense solid suspensions have been investigated [4-6], practical applications of these models have never been realized. In this report, we present a study that examines the dependence of scattering and phase-velocity measurements on soilds concentration. The study covers model analyses and laboratory measurements and also proposes a practical method for monitoring solids concentration.

2 VISCOSITY MEASUREMENT

In this section, we first present a complete description of the ANL ultrasonic viscometer and its performance, followed by results of wedge-material evaluation and a proposed technique for low-viscosity measurement. Preliminary results are also presented, along with an assessment of the measurement accuracy and stability, which may be affected by the presence of suspended particles.

2.1 The ANL Ultrasonic Viscometer

ANL's ultrasonic viscometer is a nonintrusive in-line device that measures both fluid density and viscosity. The principle of the viscometer is based on acoustic- and shear- impedance measurements, a technique first applied by Moore and McSkimin [7] to measure dynamic shear properties of solvents and polystyrene solutions. Incident ultrasonic shear (1-10 MHz) and longitudinal waves (1 MHz) are launched to two wedge surfaces that are in contact with the fluid, and their reflections are measured. The reflection coefficients, along with sound speed in the fluid, are used to calculate fluid density and viscosity. Oblique incidence was commonly used because of better sensitivity, but mode-converted waves often occur in wedges that are not of perfect crystal structure and that lack well-polished surfaces. For practical applications, we use the normal-incidence arrangement.

2.1.1 Longitudinal Waves and Acoustic Impedance of Fluid

Acoustic impedance of fluid, Z_l, is the product of fluid density, ρ, and phase velocity,V, of sound in fluid; it can be determined by measuring the reflection coefficient, R, at the boundary of the fluid and transducer wedge. If we select the normal incidence configuration, R is given as

$$R = \frac{Z_l - Z_w}{Z_l + Z_w}, \tag{1}$$

where Z_W is the acoustic impedance of the wedge in which longitudinal waves propagate from transducer to fluid. If the phase velocity in fluid can be determined accurately by other measurement (such as time-of-flight of longitudinal waves traveling in the fluid), the fluid density can be derived from

$$\rho = \frac{Z_w(1-|R|)}{V(1+|R|)}, \tag{2}$$

where the absolute value of the reflection coefficient is used because in principle R is a complex number. However, in practice, if we assume that wave attenuation in the wedge and fluid can be neglected, only the real parts of R and Z_W are used in the density calculation.

2.1.2 Shear Waves and Shear Impedance of Fluid

Use of the ultrasonic shear reflectance method to obtain the shear mechanical properties of fluids has been the subject of many studies for Newtonian [8] and non-Newtonian [9] fluids. Consider that gated shear-horizontal (SH) plane waves propagate in a wedge at an angle normal incident to the polished surface that is in contact with the fluid and are reflected back. The shear reflection coefficient can be expressed as given in Eq. 1 with shear impedances replacing acoustic impedances. The shear impedances of the wedge, Z_{WS}, and fluid, Z_{lS}, are given as

$$Z_{ws} = \sqrt{\rho_w C_{44}} \tag{3}$$

$$Z_{ls} = \sqrt{j\omega\rho\eta} \quad , \tag{4}$$

where ρ_W is the density of the wedge material, C_{44} the stiffness constant of the wedge, ω the radial frequency of the shear wave, and η the fluid viscosity. Using Eq. 4, we have assumed that the fluid behaves as a Newtonian fluid; more complex expressions are expected for non-Newtonian fluids[10]. The shear impedance of fluid is a complex value consisting of amplitude and phase. The phase change is very small for a single reflection, so we consider only the amplitude variation. The shear reflection coefficient, R_s , which is a measurable quantity, can be used to calculate the density-viscosity product by

$$\sqrt{\rho\eta} = \sqrt{\frac{\rho_w C_{44}}{2\omega}} \frac{1-\sqrt{1-2K^2}}{K} \quad , \tag{5}$$

where $K = (1-|R_S|^2)/(1+|R_S|^2)$.

Equation 5 predicts the measurement sensitivity and range of the shear reflectance method. Figures 1 and 2 show the dependence of reflection coefficient on density-viscosity product for various operating shear frequencies and wedge materials, respectively. In principle, lower-shear-impedance materials and higher operating shear frequencies provide better sensitivity but smaller measurement range. However, for tank-waste applications, the choice of Lucite and 10 MHz is not sufficient to achieve the desired sensitivity.

2.1.3 Viscometer Design

Figure 3 shows the basic design of the ultrasonic viscometer and its signal processing scheme. The basic design consists of two transducer wedges mounted on a pipe opposite one another and flush with the inner surface of the pipe. The wedge uses an offset surface to provide the reference

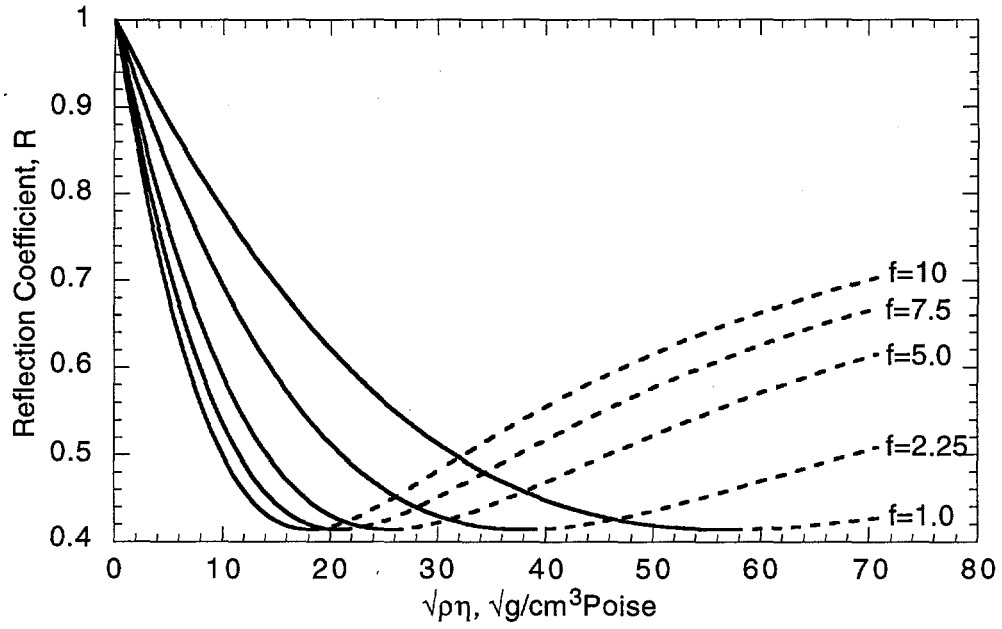

Fig. 1. Reflection coefficient as a function of fluid density-viscosity product for various operating shear wave frequencies.

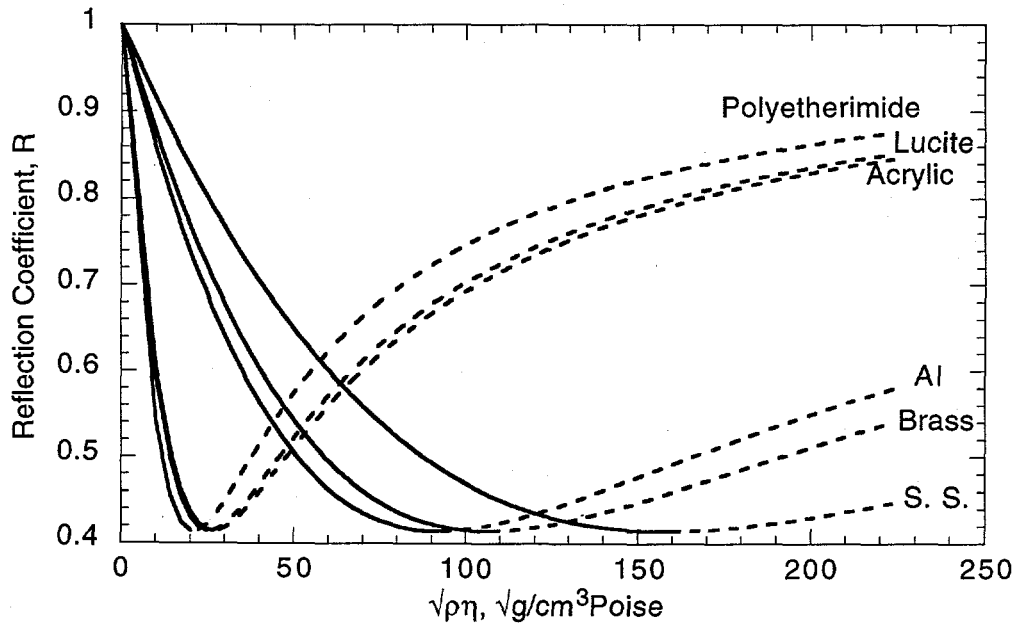

Fig. 2. Reflection coefficient vs. square root of fluid density-viscosity product for various wedge materials (S.S. = stainless steel).

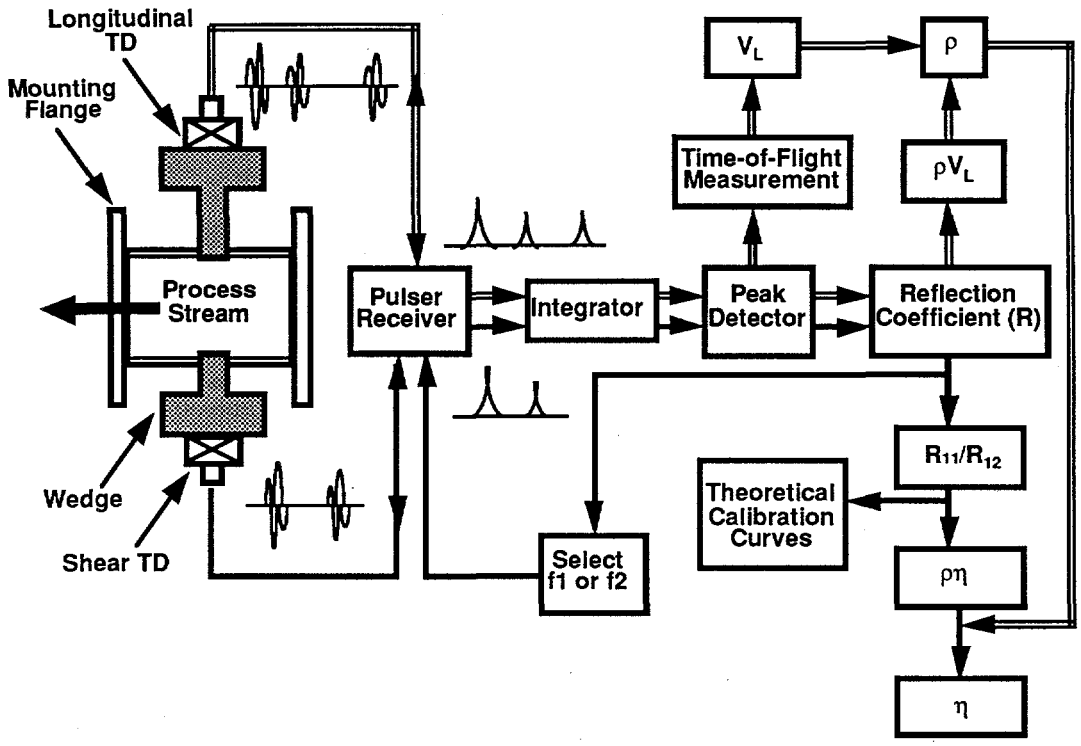

Fig. 3. Experimental configuration and setup for viscometer.

reflection that is compared with the reflection from the sensing surface to give the reflection coefficient measurement. In effect, the offset surface provides a continuous reference signal for self-calibration. Two types of transducer, shear and longitudinal, are used; both operate under the pulse-echo mode. Three major reflections are detected for longitudinal-wave operation, corresponding to reflections from the offset surface, the sensing surface that is in contact with the fluid, and the pipe wall on the opposite side. The amplitude ratio of the first two reflections produces a measure of reflection coefficient, while the time-of-flight between the second and the third reflections deduces the phase velocity of the longitudinal wave in the fluid. Thus, longitudinal-wave operation gives a direct measure of fluid density. Shear-wave operation detects only two reflections because most fluids do not support shear waves. The amplitude ratio of the two reflections calculates the reflection coefficient from which the density-viscosity product is deduced.

2.2 Laboratory Tests and Results

The feasibility of this technology has been demonstrated and reported [11]. The primary effort of this program is to evaluate wedge materials and determine the sensitivity and accuracy of the wedges in density and viscosity measurements. Table 1 lists the tested wedge materials and their acoustic properties. For the tests, transducers (longitudinal and shear) were attached to wedges

Table 1. Characteristics of various wedge materials

Material	Density, ρ (g/cm^3)	Longitudinal Velocity, V_L (cm/μs)	Longitudinal Impedance, ρV_L	Shear Velocity, V_{SH} (cm/μs)	Shear Impedance, ρV_{SH}	Working Temperature, T_w (°F)
ABS[a]	1.5279	0.2330	0.3560	——	——	185
Acrylic (Cast)	1.1800	0.2731	0.3222	0.1369	0.1615	200
Acrylic (Extruded)	1.1800	0.2525	0.2979	0.1369	0.1615	200
Delrin	1.0341	0.2137	0.2210	0.0931	0.0963	180
Lucite	1.2800	0.2335	0.2989	0.1119	0.1432	200
Plexiglass	1.1897	0.2701	0.3214	0.1621	0.1928	200
Polyetherimide	1.2700	0.2403	0.3052	0.1041	0.1323	338
Polystyrene	1.0279	0.2042	0.2099	——	——	170
WTD[b]	1.2624	0.2352	0.2969	0.1016	0.1283	350
HTD[b]	1.4038	0.2591	0.3637	0.1127	0.1582	500
VHTD[b]	1.4315	0.2309	0.3305	0.0985	0.1409	900

[a]ABS: Acrylonitrile-butadiene-styrene.

[b]Delay lines are supplied by Panametric, Inc., for high-temperature applications. WTD = moderate-temperature delay line; HTD = high-temperature delay line; VHTD = very-high-temperature delay line.

with epoxy. They are excited by a wideband pulse and generate pulses having a center frequency of 1 MHz for longitudinal waves and 5 MHz for shear waves. Reflections from the two surfaces of each wedge are rectified and integrated. The integrated reflection amplitudes are used to calculate the reflection coefficients. Typically, 500 averages are applied to the signals to reduce the signal-to-noise ratio.

2.2.1 Density Measurement

The longitudinal-wave reflectance method is used to measure fluid density. Table 2 lists the liquids of density standard used in the test for density calibration. The longitudinal-wave phase velocity in each liquid, deduced from time-of-flight measurement, is also given. Note that variation in phase velocity of the standard liquids does not correlate with their density change; thus, phase velocity alone cannot be used to predict liquid density. However, by combining phase velocity and *acoustic* impedance measurements, we can obtain an accurate measurement of liquid density. Figure 4 shows the density calibration results for two wedge materials, polyetherimide and

Table 2. Liquids used for density calibration tests

Liquid*	Chemical Constituents	Density (g/cm^3)	Longitudinal-Wave Phase velocity (cm/μsec)
R-827	Kerosene Chloronaphthlene Napthol	0.818	0.12766
G-1000	2-Butoxy Ethanol 51.9% Ethylene Glycol 47.2% BASACID Green <1%	1.002	0.15906
Y-120	Chloronaphthlene 99% Kerosene <1% Mono Azo Dye <1%	1.194	0.14272
B-175	Diazene-42 99% Diazene-200 <1% Solvent Blue 36 <1%	1.730	0.11452

*Supplied by ALTA Robbins, Anaheim, CA.

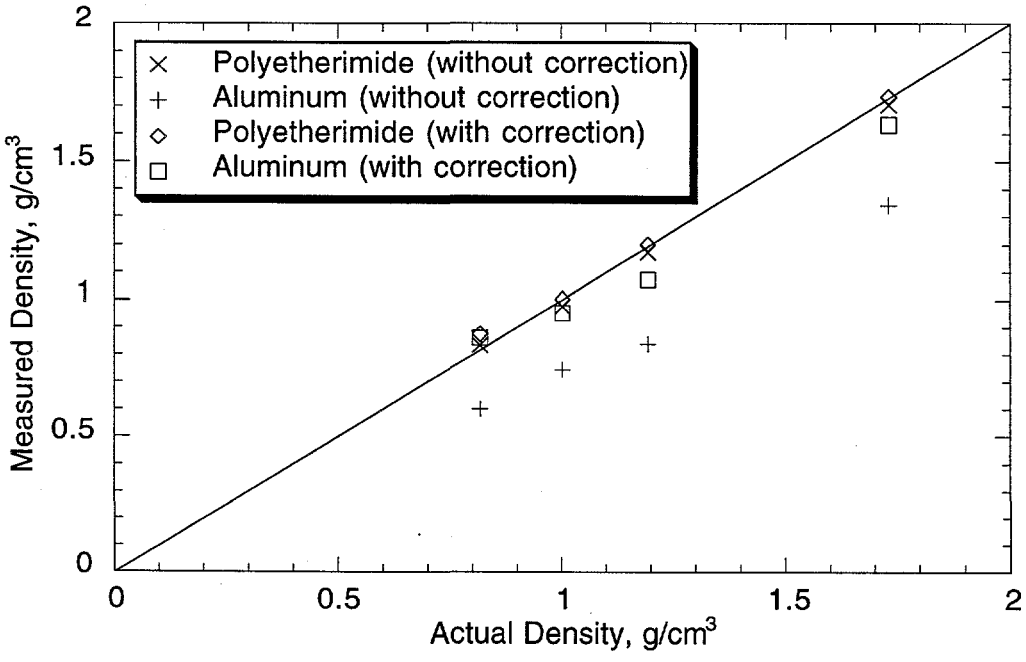

Fig. 4. Density calibration results for two wedge materials, polyetherimide and aluminum. A wedge correction function of 4% is determined.

aluminum. The polyetherimide wedge gives an accuracy better than 0.5% for the test liquids, but results from the aluminum wedge are significantly lower than the actual values. The discrepancy of the aluminum wedge may be due to wetting problems and wedge geometry, which consistently give a 4% higher reflection coefficient measurement. If we apply the 4% correction to both wedges, which have the same design, the discrepancy is significantly reduced (as shown in Fig. 4).

2.2.2 Viscosity Measurement

In comparison with the density wedge, the wedge design for viscosity measurement is scaled down in a ratio of longitudinal to shear velocities. Earlier measurements [11] show that an aluminum wedge gives about a 1% reflection amplitude change for a 250-cP viscosity change. This sensitivity is very poor, especially for low-viscosity measurement, but can be improved if a low-impedance wedge and high operating frequency are used. Figure 5 shows the reflection coefficients as a function of viscosity for the polyetherimide wedge at two frequencies. In the high-viscosity range, better sensitivity is obtained at the higher frequency (10 MHz). We performed the calibration tests for three low-impedance wedge materials, polyetherimide, acrylic (Lucite), and polystyrene. Table 3 lists the liquids used for the calibration tests; note that all of the liquids have a similar density but vary in viscosity. Figure 6 shows the calibration results. Lucite shows the best among the three as a wedge material for viscosity measurement. However, all of the measured viscosities are lower than their expected values. The discrepancy may be attributed to non-Newtonian fluid behavior [12], surface wetting, and poor sensitivity.

For low-viscosity liquids, the technique based on measurement of impedance (or reflection coefficient) requires improved detection sensitivity. One improvement approach is to monitor multiple reflections because each echo represents one interaction at the wedge/liquid boundary. To obtain multiple echoes, the wedge design must be modified. Two design factors should be considered, echo interference and signal attenuation. The simplest design is to use a thin-plate configuration. A thin polyetherimide plate was fabricated and tested with glycerol-water solutions. In Fig. 7, we show the measured results derived from the second and third echoes over a viscosity range of 5 to ≈600 cP. The derived viscosities in Fig. 7 are calculated from the measured reflection coefficients by using Eq. 5, in which R_s is replaced by $(R_s)^{1/n}$ where n is the echo number. It is evident that multiple reflections improve measurement sensitivity, and thus low-viscosity liquids can be monitored with this technique.

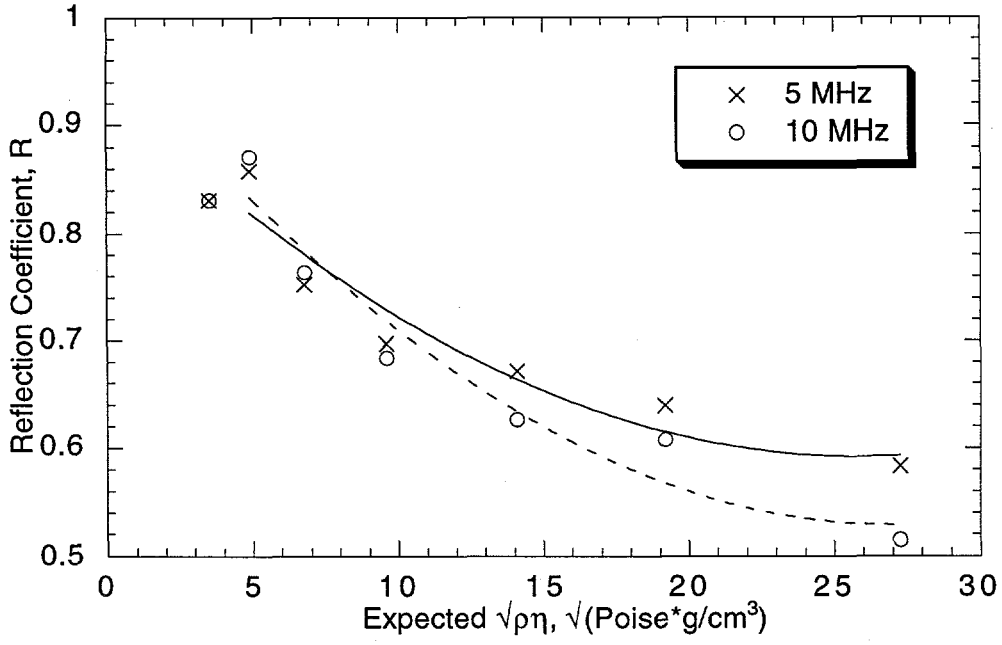

Fig. 5. Measured reflection coefficients with a polyetherimide wedge at two operating frequencies.

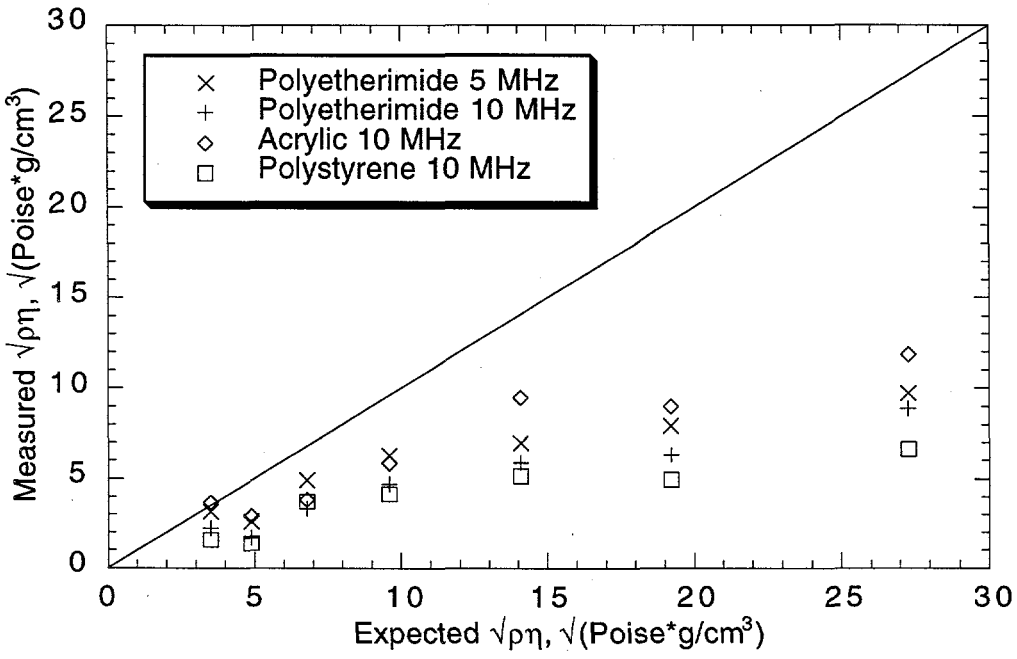

Fig. 6. Viscosity calibration data for various wedge materials.

Table 3. Liquids used for viscosity calibration tests

Liquid*	Chemical Constituent	Density (g/cm^3)	Viscosity (cP)
N600	Mineral oil	0.8876	1381
N1000	PAO oil	0.8479	2823
N2000	Poly(1-butene)	0.8753	5248
N4000	Poly(1-butene)	0.8812	10450
N8000	Poly(1-butene)	0.8873	22390
N15000	Poly(1-butene)	0.8919	41360
N30000	Poly(1-butene)	0.8954	83040

*Supplied by Cannon Instrument Company, State College, PA.

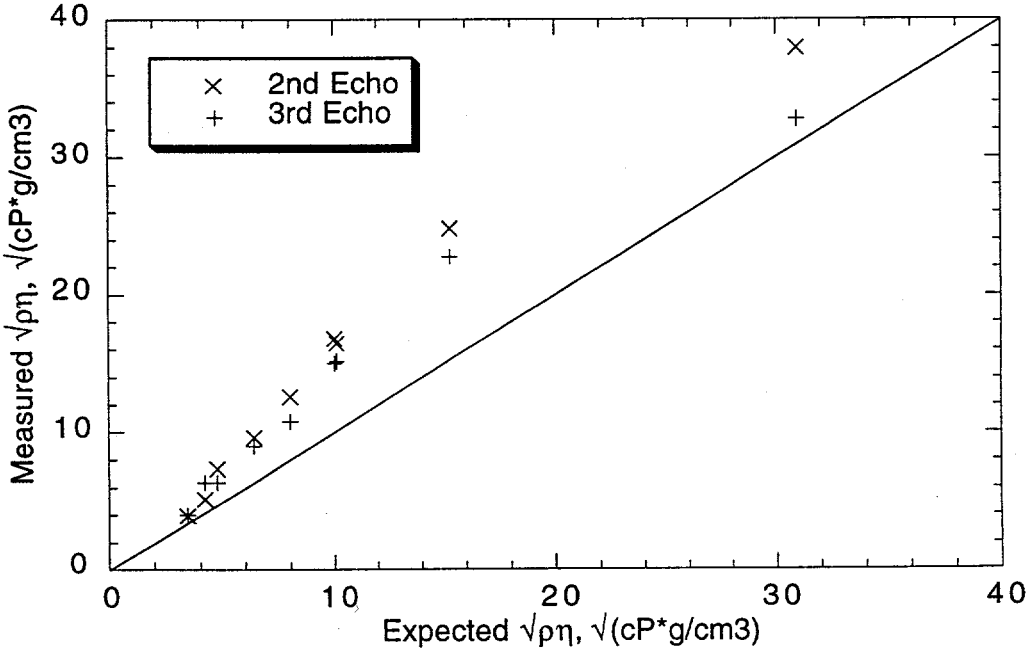

Fig. 7. Viscosity calibration data in low-viscosity range obtained with polyetherimide wedge and multiple reflection technique.

2.2.3 Errors and Limitations

Measurement errors in both density and viscosity can be estimated by the following relationships. For density measurement based on the longitudinal-wave reflection coefficient, R_L, the error is given by

$$\frac{\Delta\rho}{\rho} = \frac{2R_L}{1-R_L^2}\frac{\Delta R_L}{R_L} \quad . \tag{6}$$

Equation 6 delineates the nonlinear amplification effect between the measurement error in reflection coefficient and the prediction error in density. In particular, when R_L is near unity, accurate density measurement is almost impossible. For viscosity measurement, the theoretical error can be estimated from

$$\frac{\Delta\eta}{\eta} = \frac{4R_S}{1-R_S^2}\frac{\Delta R_S}{R_S} \quad . \tag{7}$$

Similarly, measurement accuracy depends on the reflection coefficient. Figure 8 shows the theoretical measurement errors of density and viscosity, based on Eqs. 6 and 7, as functions of the reflection coefficients of the longitudinal and shear waves, respectively. For wedges of high shear impedance, which causes a large impedance mismatch with most liquids of interest, the viscosity measurement not only lacks sensitivity but also introduces a large measurement error. Selection of a proper wedge material is the critical step in reflection-coefficient measurement.

2.2.4 Effective Viscosity of Suspensions

Because of viscous drag on a particle, the presence of particles in a fluid distorts the flow and increases shear resistance. Assuming no mutual hydrodynamic interaction, Einstein [13] derived an effective viscosity, η_{eff}, in terms of solid volume concentration φ, given as

$$\eta_{eff} = \eta\,(\,1 + 2.5\varphi\,)\,, \tag{8}$$

where 2.5 is a shape factor for spherical particles. For higher solids concentrations, for which one must consider hydrodynamic interactions in the suspension, Vand [14] obtained for spheres

$$\eta_{eff} = \eta\,(\,1 + 2.5\varphi + 7.349\varphi^2\,)\,. \tag{9}$$

The effective viscosity is a bulk phenomenon that affects flow dynamics. Our ultrasonic viscometer measures fluid viscosity at the fluid/wedge interface; therefore, the bulk phenomenon cannot be measured and the relationships given in Eqs. 8 and 9 cannot be verified.

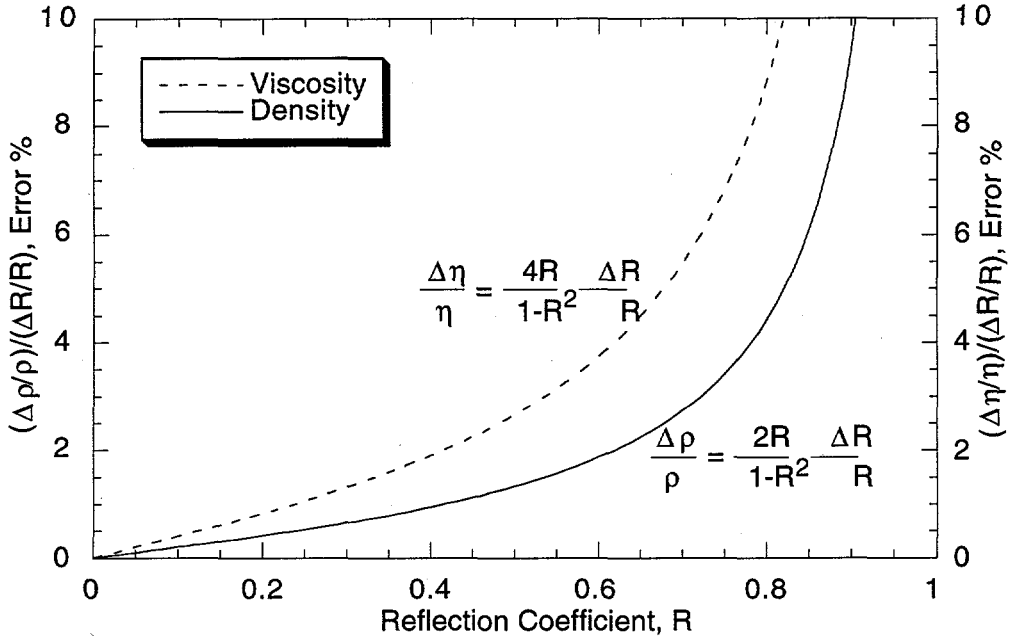

Fig. 8. Theoretical measurement errors of density and viscosity as function of reflection coefficient.

3 Measuring Volume Percent of Solids

The second goal of this project is to develop an on-line ultrasonic sensor for measuring volume percent of solids. Limited work to date has shown that for solids concentrations of <15%, volume percent of solids can be correlated with ultrasonic attenuation. However, absolute attenuation is difficult to measure, and relative attenuation change requires a reference. Thus, the technique can at best apply to diagnostic monitoring. Use of phase- velocity variation for solids measurement has frequently been suggested. Various theoretical models [15] have been reported and available data show some dependence of phase-velocity variation on solids concentration up to 30 vol.%. But due to limited experimental data, the models cannot be realistically assessed. In this section, we summarize the theoretical models, present some preliminary data, and propose a sensor design.

3.1 Theoretical Models

The problem of wave propagation and scattering in random media [16] is important to every field of science and engineering, for example, communication and remote sensing in the atmosphere, biological imaging, and geological oil exploration. However, rigorous formulation for this problem does not exist and is mathematically impossible. To understand the problem, one must rely on simplified geometries or on models based on statistical averaging or a phenomenological approach. For the present problem (ultrasonic wave propagation in suspensions), three models [17] are being proposed and investigated: (a) effective medium approach, (b) coupled-phase model, and (c) multiple scattering treatment.

3.1.1 Effective Medium Approach

The effective medium approach is a phenomenological approach that assumes that in a suspension there will be a well-defined phase velocity, V, depending on an effective density, ρ_{eff}, and an effective compressibility, β_{eff}, given as

$$V = (\rho_{eff}\,\beta_{eff})^{-1/2}. \tag{10}$$

The effective compressibility commonly used is a simple averaging,

$$\beta_{eff} = \varphi\beta_2 + (1 - \varphi)\beta_1, \tag{11}$$

where 1 and 2 represent fluid phase and solid, respectively. There are, however, different ways of averaging the density depending on the assumption chosen. The simplest expression used by Urick [18] is

$$\rho_{eff} = \varphi\,\rho_2 + (1-\varphi)\,\rho_1 . \tag{12}$$

Ament [19] considers the effect of fluid viscosity and particle size, a, and obtains

$$\rho_{eff} = \varphi\rho_2 + (1-\varphi)\rho_1 - 2(\rho_2-\rho_1)^2\varphi(1-\varphi)Q/(Q^2+U^2), \tag{13}$$

where

$$Q = 2(\rho_2-\rho_1)(1-\varphi) + \frac{9\delta}{2a}\rho_1 + 3\rho_1 \tag{14}$$

and

$$\begin{aligned} \delta &= \sqrt{2\eta/\omega\rho_1}, \\ U &= \frac{9}{2}\rho_1\left[(\delta/a) + (\delta/a)^2\right]. \end{aligned} \tag{15}$$

For a suspension with a large volume fraction of suspended particles, Biot [20] developed a theory by treating the medium as a porous solid. The theory gives for the effective density

$$\frac{1}{\rho_{eff}} = \frac{(1-\varphi)\varphi\rho_2 + (\tau - 2\varphi + \varphi^2)\rho_1}{\tau\rho_1\left[\varphi\rho_2 + (1-1/\tau)(1-\varphi)\rho_1\right]}, \tag{16}$$

where τ is a parameter called "tortuosity." Two expressions are suggested for τ: $(2-\varphi)/2(1-\varphi)$ or $(3-\varphi)/2$.

3.1.2 Coupled-Phase Model

This model is based on analysis of a two-phase fluid by solving four differential equations that govern the motion of the two-phase mixture. The solution gives for the effective wave number, k,

$$k^2 = \omega^2\left[(1-\varphi)\beta_1 + \varphi\beta_2\right] \times \frac{\rho_1\left[\rho_2(1-\varphi+\varphi S) + \rho_1 S(1-\varphi)\right]}{\rho_2(1-\varphi)^2 + \rho_1\left[S + \varphi(1-\varphi)\right]}, \tag{17}$$

where S, defined in Eqs.18 and 19, is a complex quantity that corresponds to an attenuated wave:

$$S = R + iU/2\rho_1 \tag{18}$$

and

$$R = \frac{1+2\varphi}{2(1-\varphi)} + \frac{9\delta}{4a} . \tag{19}$$

From the effective wavenumber, one obtains the effective wave velocity V = Re(ω/k) and attenuation α = Im(k).

Variations of phase velocity over a range of solid-volume percentages are calculated for the above models for two types of particles, glass beads and kaolins (their acoustic impedances are 21.12 x 10^5 and 10.66 x 10^5 g/cm^2-s). Calculated results are shown in Fig. 9 for glass beads and in Fig. 10 for kaolins. Most models except Biot-2 show decreasing phase velocity at lower volume fractions, then increasing phase velocity at higher volume fractions.

3.1.3 Multiple Scattering Treatment

The widely used multiple scattering treatment was developed by Waterman and Truell [21] and Twersky [22]. The treatment is based on an approximation in which the exciting field seen by a scatterer may be represented by the total field that would exist at the scatterer if the scatterer were not present. Furthermore, it assumes that scatterers are statistically independent, i.e., the probability of finding a scatterer at one point is independent of other scatterers. The treatment yields an expression for the effective wavenumber in terms of single-particle scattering amplitudes, which is given as

$$\left(\frac{k}{k_0}\right)^2 = \left[1+\frac{2\pi N}{k_0^2} f(0)\right]^2 - \left[\frac{2\pi N}{k_0^2} f(\pi)\right]^2, \tag{20}$$

where k is the effective wavenumber, k_0 is the propagation wavenumber in the fluid, and f(0) and f(π) are the single-particle scattering amplitudes in forward- and backward-direction, respectively. Considering scattering by a spherical particle, the scattering amplitude can be given as

$$f(\theta) = \frac{i}{2k_o}\sum_{m=0}^{\infty}(2m-1)(1+\Re_m)p_m(\cos\theta), \tag{21}$$

where $\Re_m$ is a reflection coefficient at the particle surface, and is defined as

$$\Re_m = \frac{h_m'^*(k_0a)+i\chi_m h_m^*(k_0a)}{h_m'(k_0a)+i\chi_m h_m(k_0a)}, \tag{22}$$

where $h'_m = j'_m + i\,\eta'_m$, $h_m = j_m + i\,\eta_m$, and h'^*_m, h^*_m are the complex conjugates of h'_m, h_m, respectively. j_m and η_m are the m-th order spherical Bessel and Neumann functions, respectively. χ_m is a constant derived from the boundary conditions at the particle surface, which has the form of [23]

$$\chi_m = i\frac{\rho C}{\rho_e C_e}\frac{j_m'(k_e a)}{j_m(k_e a)}, \tag{23}$$

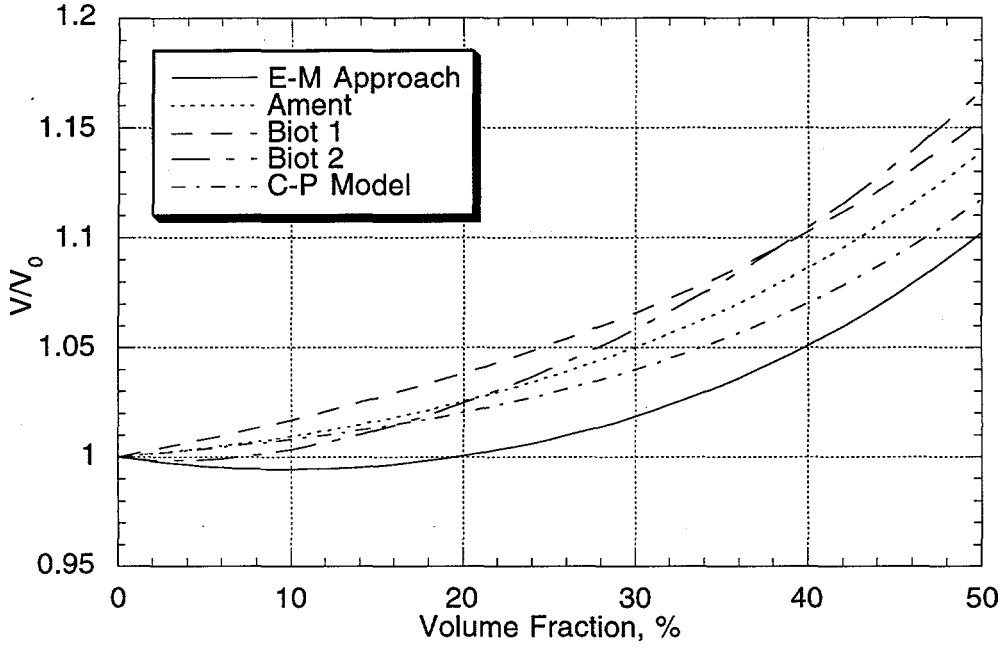

Fig. 9. Model calculations of phase velocity vs. volume fraction for glass beads.

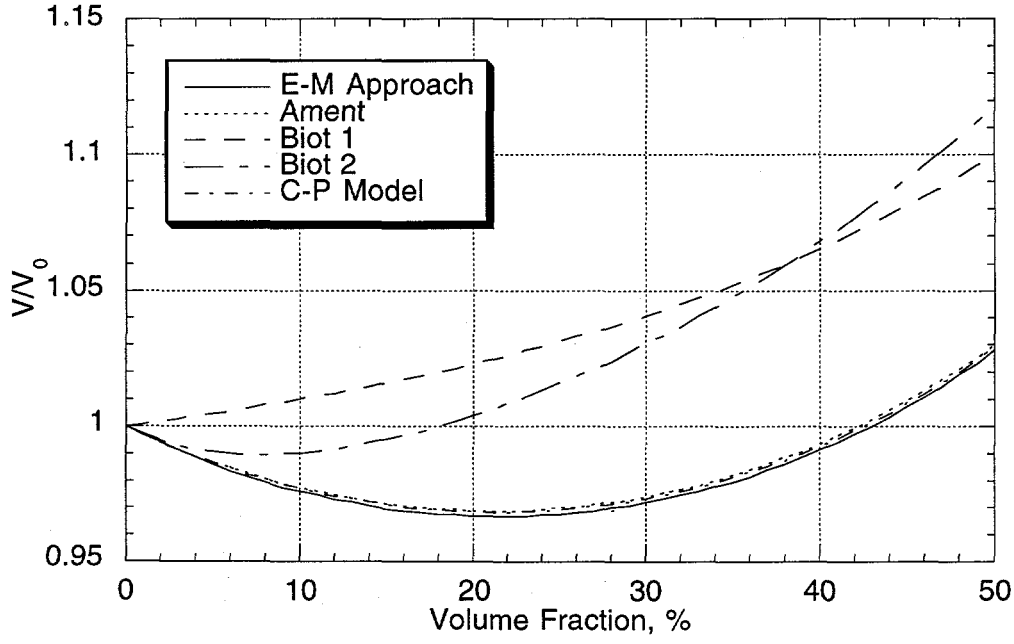

Fig. 10. Model calculations of phase velocity vs. volume fraction for spherical kaolins.

where ρ_e, C_e, and k_e are the density, phase velocity, and wave number of the spheres having a diameter of a. ρ and C are density and phase velocity of the fluid. The phase velocity of the sphere can be calculated with Eq. 10. In effect, Eq. 23 considers only the acoustic properties of the spheres; thermal and viscous effects are not included. For rigid spheres, χ_m approaches zero.

In general, k in Eq. 20 is a complex value defined as

$$k = k_R + i\alpha, \tag{24}$$

where $k_R = \omega/V$ (the real part of the modified wave number), and α is attenuation. Substituting Eqs. 21 and 23 into Eq. 20, we obtain two coupled equations, Eqs. 24 and 25, which can be solved for sound velocity (V) and attenuation (α):

$$\frac{k_R^2 - \alpha^2}{k_o^2} = 1 + \frac{3\varphi}{k_o^2 a^3} f_R(0) + \frac{9\varphi^2}{4k_o^4 a^6}[f_R^2(0) - f_I^2(0) - f_R^2(\pi) + f_I^2(\pi)] \tag{25}$$

$$\frac{k_R \alpha}{k_o^2} = \frac{3\varphi}{2k_o^2 a^3} f_I(0) + \frac{9\varphi^2}{4k_o^4 a^6}[f_R(0) f_I(0) - f_R(\pi) f_I(\pi)] \ , \tag{26}$$

where f_R and f_I represent the real and the imaginary part of the scattering amplitude, respectively.

The model predicts both attenuation and phase velocity in solid suspensions of spherical particles of the same size. Particles of irregular shapes show very little effect on wave propagation [18]. However, the size distribution is currently treated with statistical averaging. Details of this model will be the subject of a future report.

3.2 Experimental Results

To verify the model predictions on phase-velocity variation over a range of solid concentrations, we conducted laboratory measurements of hollow glass beads suspended in Echogel, a water-based gel that is commonly used as a transducer coupling material. The measured sound speed in the Echogel is 0.153 cm/μs,which gives a wavelength of 0.153 cm for 1 MHz longitudinal waves. The glass beads have a nominal diameter of 8 μm, or much smaller than the wavelength; thus, we are primarily measuring Rayleigh scattering, the principle of which is that the absorption cross section is inversely proportional to the wavelength and directly proportional to the volume of the particle. Measurement of the absorption cross section is still in progress. The data we present here correspond to the phase velocity measurement. Phase velocities of 1 MHz longitudinal waves were measured for solid concentrations up to 50% by volume. Figure 11 shows the data and with the model predictions. The Biot-1 model (Eq. 16) gives the best fit to the

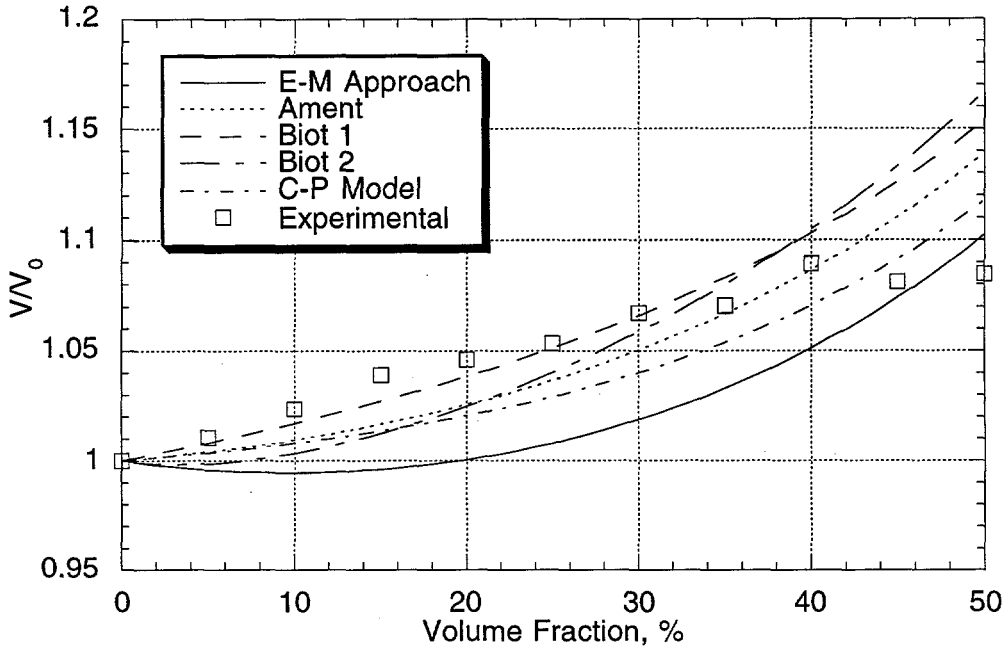

Fig. 11. Sound velocity vs. solids concentration for hollow glass beads of 8 μm suspended in Echogel, compared with theoretical prediction.

data up to ≈30 vol.% by volume. There is an approximate 5% increase in phase velocity as the particle concentration is increased to 30 vol.%. However, for concentrations higher than 30%, the measured phase velocities show very little change.

4 CONCLUSIONS

In this report, we present the results of a feasibility study, funded by DOE/EM-50 (under characterization and monitoring of tank waste), to examine two ultrasonic techniques for solid/liquid flow monitoring. The flow parameters of interest are liquid viscosity and volume percent of solids. Sensors derived from the techniques will apply to monitoring of nuclear waste in a typical nuclear-waste transporting line. The ranges of waste viscosity and solid concentration are 1-30 cP and 0-30 vol.%, respectively. The technique for viscosity measurement is based on the patented ANL ultrasonic viscometer. However, feasibility is based on application of the ANL viscometer to low-viscosity measurement. We demonstrated in this study that the ANL viscometer, based on acoustic and shear impedance measurements, can be modified for low-viscosity application. The modification involves use of a thin wedge and monitoring of multiple reflections. For solids concentration measurement, we demonstrated in the laboratory that the phase velocity of propagating ultrasonic waves in a solid suspension increases linearly with solids concentration up to 30 vol.%. Thus, a simple phase velocity measurement may provide a qualitative measurement of solids concentration. For more quantitative measurement, a scattering technique is needed. Development of a practical scattering sensor is currently in progress. Future work in this project includes (a) development of a solids concentration sensor based on a scattering technique and (b) design and testing of a prototype flow instrument that integrates both sensors.

REFERENCES

1. S. H. Sheen, W. P. Lawrence, H. T. Chien, and A. C. Raptis, "Method for Measuring Liquid Viscosity and Ultrasonic Viscometer," U. S. Patent 5,365,778, Nov. 22, 1994.

2. R. J. Urick and W. S. Ament, "The Propagation of Sound in Composite Media," J. Acoust. Soc. Amer., Vol. 21, pp. 115-119, 1949.

3. S. H. Sheen and A. C. Raptis, "HYGAS Coal-Slurry Mass-Flow Measurements Using Ultrasonic Cross-Correlation Techniques," Argonne National Laboratory Report ANL/FE-49622-TM07, 1979.

4. M. A. Biot, "Gene alized Theory of Acoustic Propagation in Porous Dissipative Media," J. Acoust. Soc. Amer., Vol. 44, pp. 1254-1264, 1962.

5. A. S. Ahuja, "Formulation of Wave Equation for Calculating Velocity of Sound in Suspensions," J. Acoust. Soc. Amer., Vol. 51, No. 3 (part 2), pp. 916-919, 1972.

6. M. C. Davis, "Attenuation of Sound in Highly Concentrated Suspensions and Emulsions," J. Acoust. Soc. Amer., Vol. 65, pp. 387-390, 1979.

7. R. S. Moore and H. J. McSkimin, "Dynamic Shear Properties of Solvents and Polystyrene Solutions from 20 to 300 MHz," Physical Acoustics, Vol. VI, pp. 167-242, 1970.

8. F. Cohen-Tenoudji, et al., "A Shear Wave Rheology Sensor," IEEE Trans. on Ultrasonics, Ferroelectrics, and Frequency Control, Vol. UFFC-34 (2), pp. 263-269, 1987.

9. G. Harrison and A. J. Barlow, "Dynamic Viscosity Measurement," Methods of Experimental Physics, Vol. 19, pp. 137-178, 1981.

10. S. H. Sheen and A. C. Raptis, "A Feasibility Study on Advanced Techniques for On-line Monitoring of Coal Slurry Viscosity," Argonne National Laboratory Report ANL/FE-87-8, 1987.

11. S. H. Sheen, H. T. Chien, and A. C. Raptis, "An In-line Ultrasonic Viscometer," Rev. of Progress in Quantitative Nondestructive Evaluation, Vol. 14A, pp. 1151-1158, 1995.

12. S. H. Sheen, H. T. Chien, and A. C. Raptis, "Measurement of Shear Impedances of Viscoelastic Fluids," 1996 IEEE International Ultrasonics Symp., to be published in 1997.

13. A. Einstein, Ann. Phys. Vol. 4, p. 289, 1906. (or L. D. Landau and E. M. Lifshitz, " Fluid Mechanics," p. 79, Pergamon Press, 1959).

14. V. Vand, J. Phys. Colloid Chem. Vol. 52, p. 277, 1948. (or A. H. Harker, et. al., "Ultrasonic Propagation in Slurries," Ultrasonics 1991, Vol. 29, pp. 427-438, 1991).

15. L. W. Anson and R. C. Chivers, "Ultrasonic Propagation in Suspensions -- A Comparision of a Multiple Scattering and an Effective Medium Approach," J. Acoust. Soc. Am., Vol. 85 (2), pp. 535-540, 1989.

16. A. Ishimaru, "Wave Propagation and Scattering in Random Media," Vols. 1 & 2, Academic Press, 1978.

17. A. H. Harker, and J. A. G. Temple, "Velocity and Attenuation of Ultrasound in Suspensions of Particles in Fluids," Phys. D, Appl. Phys. 21, pp. 1576-1588, 1988.

18. R. J. Urick, "Absorption of Sound in Suspensions of Irregular Particles," J. Acoust. Soc. Am., Vol. 20 (3), pp. 283-289, 1948.

19. W. S. Ament, " Sound Propagation in Gross Mixtures," J. Acoust. Soc. Am., Vol. 25, pp. 638-641, 1953.

20. M. A. Biot, "Theory of Propagation of Elastic Waves in a Fluid-Saturated Porous Solid -- II. Higher Frequency Ranges," J. Acoust. Soc. Am., Vol. 28, pp. 179-191, 1956.

21. P. C. Waterman and R. Truell, "Multiple Scattering of Waves," J. of Math. Phys., Vol. 2 (4), pp. 512-537, 1961.

22. V. Twersky, "On Scattering of Waves by Random Distributions -- I. Free-space Scattering Formalism," J. Math. Phys., Vol. 3 (4), pp. 700-734, 1962.

23. P. M. Morse and K. U. Ingard, "Theoretical Acoustics," Chap. 8, McGraw-Hill Co., 1968.

Distribution for ANL-97/4

Internal:

S. Ahuja	J. Jendrzejczyk	A. C. Raptis
S. Bakhtiari	E. R. Koehl	S.-H. Sheen (20)
H.-T. Chien	D. S. Kupperman	J. G. Sun
S. Dieckman	W. P. Lawrence	R. A. Valentin
W. A. Ellingson	C. A. Malefyt	R. W. Weeks
N. Gopalsami	R. B. Poeppel	TIS Files

External:

DOE-OSTI for distribution per UC-606 (123)
ANL Libraries
    ANL-E
    ANL-W
Manager, Chicago Field Office, DOE
Energy Technology Division Review Committee:
    H. K. Birnbaum, University of Illinois, Urbana
    R. C. Buchanan, University of Cincinnati, Cincinnati, OH
    S.-N. Liu, Fremont, CA
    H. S. Rosenbaum, Fremont, CA
    R. K. Shah, University of Kentucky, Lexington
    S. Smialowska, Ohio State University, Columbus
    R. E. Smith, Altran Corp., Huntersville, NC
C. Purdy, USDOE, Germantown, MD
T. Thomas. Lockheed Martin Idaho Technologies, Idaho Falls
P. Wang, Special Technologies, Santa Barbara, CA 93111
S. Wyrick, Science Applications International Corp., Gaithersburg, MD